Elasticity of α-Helical Coiled Coils

Charles W. Wolgemuth[1] and Sean X. Sun[2]

[1]*Department of Cell Biology and Center for Cell Analysis and Modeling, University of Connecticut Health Center, Farmington, Connecticut 06030-3505, USA*

[2]*Department of Mechanical Engineering and Department of Chemical and Biomolecular Engineering, Johns Hopkins University, Baltimore, Maryland 21218, USA*

(Received 6 June 2006; published 15 December 2006)

Predicting large scale conformations of protein structures is computationally demanding. Here we compute the conformation and elasticity of double-stranded coiled coils using a simple coarse-grained elastic model. By maximizing the contact between hydrophobic residues and minimizing the elastic energy, we show that the minimum energy structure of a coiled coil is a supercoiled double helix of α helices. For realistic binding energies, the elastic energy of the α helices requires binding every 7th residue, which leads to a pitch and helix angle for the structure that is consistent with experimental measurements. Analysis of the model equations shows how the pitch varies with the helical repeat of the hydrophobic residues and with the ratio of the twisting modulus to the bending modulus and provides an estimate of the persistence length of around 150 nm, in agreement with previous experimental estimates.

DOI: 10.1103/PhysRevLett.97.248101 PACS numbers: 87.14.Ee, 87.15.Aa, 87.15.Cc, 87.15.La

Protein function is strongly coupled to structure. Determining a protein's structure from its sequence, however, requires extensive computation. For instance, predicting the pitch of α helices in α-helical coiled coils starting from molecular interactions is nontrivial [1–3]. Crick suggested a purely geometric parametrization of the coiled coil that describes the conformation in terms of the geometry of the α helices but leaves the α-helix pitch as a free parameter [4]. By assuming that the α helices are bent around each other without twisting about the α-helix center lines, Fraser and MacRae introduced the following relation for the coiled-coil pitch P [5]:

$$P = \frac{2\pi}{\Delta t}[h^2 - (r_0 \Delta t)^2]^{1/2}, \tag{1}$$

where r_0 is the radius of the coiled coil, h is the axial rise per amino acid, and Δt is the α-helical versus sequenced derived twist differential. This relation ignores the deformation energy of the α helix and assumes that the energetic cost for bending an α helix is much smaller than the energetic cost for twisting. Recently, elastic properties of α helices have been examined. It was suggested that the twist modulus is approximately one-half of the bending modulus [6]. In this Letter, we show that the structural properties of the coiled coil can be computed starting with an elastic rod model for the α helices.

All proteins are largely made of common secondary structural motifs such as α helices and β sheets. Elastic properties of secondary structures are important for describing conformational transitions. For example, a β sheet in F_1-ATPase bends and stores energy upon ATP binding; the stored energy is released during a recoil power stroke after ATP hydrolysis, generating torque [7]. An α helix is a helical arrangement of amino acid residues where the backbone atoms are stabilized by hydrogen bonds and the residue side chains extrude and interact with the surroundings (Fig. 1). A typical α helix has a helical pitch of 0.6 nm and ≈ 3.6 residues per turn of the helix [8,9]; residues are separated by $h = 0.6$ nm/3.6 along the helix center line axis. The circumferential angle between neighboring residues θ_1 is $2\pi/3.6$ (Fig. 1). The helix torsion is the angle between neighboring residues divided by the helix center line distance, $\tau_1 = \theta_1/h$. Molecular dynamics simulations showed that the persistence length of α helices in water ℓ_b is largely sequence independent and is 80–100 nm [6]. However, experimental estimates of the persistence length of a coiled coil (a supercoiled bundle of two α helices) give largely varying values, ranging from 25 to 150 nm [10–12]. It would seem that the rigidity of two conjoined elastic filaments should be at least twice that of a single unit. Therefore, the persistence length of a coiled coil should be 160–200 nm. We propose to compute the structure and persistence length of the coiled coil using an elastic model.

We describe the conformation of a single α helix by the center line of the helix axis, as opposed to using the conformation of the backbone atoms. Given the positions of the atoms in the helix, the position of the helix axis $\mathbf{r}(s)$ can be defined, where s is the contour length of the rod. The elastic energy of the helix can be modeled as [6,13]

$$E_0 = k_B T \int_0^L ds \frac{\ell_b}{2}\kappa^2(s) + \frac{\ell_t}{2}(\tau(s) - \tau_1)^2, \tag{2}$$

where κ is the curvature and τ is the twist density of the helix axis. ℓ_b is 80–100 nm for α helices in water, and the twist persistence length ℓ_t is roughly $\ell_b/2$. The α helix also can stretch; however, the stretch modulus is quite large and is neglected in the present treatment [6].

When two α helices are in close contact, the side chains of the helices interact and pack into a structure that has

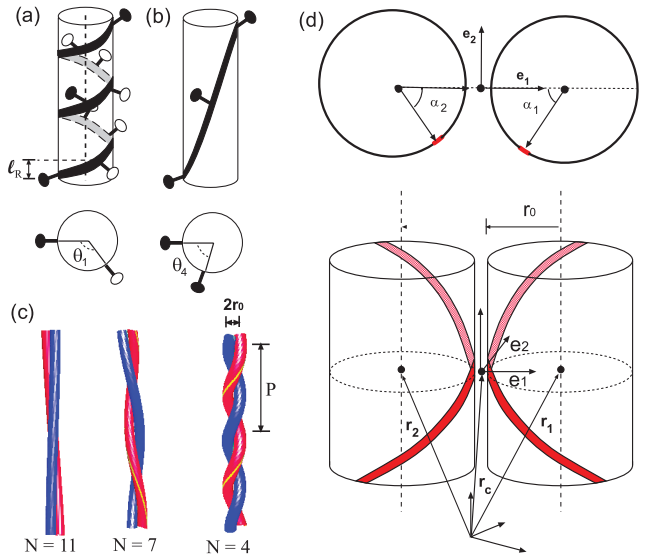

FIG. 1 (color). (a) Diagram showing a single α helix. The ribbon follows the helix backbone. The dashed line shows the helix axis, and the cylinder represents the elastic rod defined by the α helix. The lollipop shapes represent the residue side chains. The helix axis arclength distance between residues is h. The circumferential angle between the bottommost residue and its nearest neighbor is defined as θ_1. If every 4th residue (shaded black) binds to a neighboring residue on a second α helix, an effective torsion τ_4 can be defined using the angle between those residues θ_4, divided by the arclength between them $\tau_4 = \theta_4/4h$ (b). (c) The coiled-coil conformation when every 11th, 7th, and 4th residue bind. The pitch P and the distance between the α-helix center lines $2r_0$ are shown. (d) Schematic of the mathematical representation of the two α helices. Vectors $\mathbf{r}_1$ and $\mathbf{r}_2$ define the center line of each helix.

been described by Crick as "knobs into holes," where every 7th residue packs into the hole created between the first and fourth residues on the neighboring helix [8,9]; however, 11th residue repeats have also been observed [14]. Though the "heptad" hydrophobic pattern of residues is ubiquitous, it is interesting to form a general model that explores coiled-coil conformation for any hydrophobic repeat. We define the angle between a residue and its Nth neighbor to be θ_N and require that this angle be in the range between $-\pi$ and π (Fig. 1). The effective torsion between a residue and its Nth neighbor is $\tau_N = \theta_N/Nh = \Delta t/h$. Maximizing the binding energy favors the binding of every residue. However, since the residues are arranged in a helical fashion, to bind every residue requires bending and twisting of the α helix. The total energy is therefore a competition between binding and elastic deformation. The optimal configuration must have the largest number of bound residues (smallest N) while minimizing the elastic deformation (smallest τ_N). As shown in Table I, the smallest values of N for which there are minimal values of the elastic deformation energy are $N = 4$, 7, and 11.

To model the elasticity of the composite structure of two bound α helices, we define the position of the center line of the coiled coil $\mathbf{r}_c(s)$ and an orthonormal material frame triad $(\mathbf{e}_1(s), \mathbf{e}_2(s), \mathbf{e}_3(s))$, where s is the arclength along the coiled-coil axis and $\mathbf{e}_1$ is defined to point toward one of the α helices. The strain vector $(\Omega_1(s), \Omega_2(s), \Omega_3(s))$ describes the rotation of the orthonormal frame with changes in arclength, $\partial \mathbf{e}_i/\partial s = \mathbf{\Omega} \times \mathbf{e}_i$. Figure 1(d) depicts the geometry of the double-stranded coiled coil. The centers of the α helices are described by positions $\mathbf{r}_1(s)$ and $\mathbf{r}_2(s)$. We model the hydrophobic residues as a continuous helical strip on the surface of the cylinder. The position of the hydrophobic strip on helix 1 is specified by the angle α_1 between the strip and $-\mathbf{e}_1$. α_2 is the angle between the strip on helix 2 and $\mathbf{e}_1$ [see Fig. 1(d)]. Therefore,

$$\mathbf{r}_1 = \mathbf{r}_c + r_0\mathbf{e}_1; \qquad \mathbf{r}_2 = \mathbf{r}_c - r_0\mathbf{e}_1. \tag{3}$$

The binding energy between the α helices is dependent on the overlap between the two hydrophobic strips. If every Nth residue binds and the binding energy is strong enough to hold the coiled coil together, the hydrophobic interaction energy between α helices is

$$E_I = -\frac{k_B T \epsilon_R L}{Nh}, \tag{4}$$

where L is the contour length of the α-helix axis and ϵ_R is a constant that defines the binding energy per residue. Thus, the combined energy of the coiled coil is then

$$E = E_0[\mathbf{r}_1(s)] + E_0[\mathbf{r}_2(s)] + E_I, \tag{5}$$

where $E_0[\mathbf{r}_1(s)]$ is given by Eq. (2), and, to account for arbitrary hydrophobic repeat, τ_N is used in place of τ_1. $E_0[\mathbf{r}_2(s)]$ is the same energy specified by the curvature and twist density of helix 2.

To simplify the problem, we assume that the α helices are indistinguishable: Changes in arclength along one helix must equal the changes in arclength along the other

$$\frac{\partial \mathbf{r}_1}{\partial s} \cdot \frac{\partial \mathbf{r}_1}{\partial s} = \frac{\partial \mathbf{r}_2}{\partial s} \cdot \frac{\partial \mathbf{r}_2}{\partial s} = 1 + r_0^2\Omega_3^2 \equiv g, \tag{6}$$

and $\alpha_1 = \alpha_2 = \alpha$ (see Fig. 1). Equation (6) requires that $\Omega_2 = 0$, which is equivalent to assuming that the α helices are inextensible and do not slide along the residue bonds in the direction tangent to the coiled-coil axis. The curvatures and twist densities of the helices are

TABLE I. The effective torsion of the coiled coil τ_N for hydrophobic repeats between 1 and 11. Values are in nm^{-1}.

τ_1	τ_2	τ_3	τ_4	τ_5	τ_6	τ_7	τ_8	τ_9	τ_{10}	τ_{11}
10.47	−8.38	−2.09	1.05	2.93	−2.09	−0.30	1.05	2.09	−0.84	0.19

$$\kappa_{1,2}^2 = \frac{1}{g}\Omega_1^2 \mp \frac{2r_0}{g^2}\Omega_1\frac{\partial\Omega_3}{\partial s} + \frac{r_0^2}{g^2}\Omega_3^4 + \frac{r_0^2}{g^3}\left(\frac{\partial\Omega_3}{\partial s}\right)^2, \quad (7)$$

$$\tau_i = \frac{1}{\sqrt{g}}\frac{\partial\alpha}{\partial s} + \frac{1}{g}\Omega_3. \quad (8)$$

To solve for the equilibrium configuration of the coiled coil in the strong binding limit ($\alpha = 0$), we derive the Euler-Lagrange equations for Ω_1 and Ω_3, which leads to two coupled equations that define the moments M_1 and M_3 along the coiled-coil axis:

$$M_1 = \frac{2k_BT\ell_b\Omega_1}{g^{1/2}},$$
$$\frac{M_3 - r_0^2\Omega_3F_3}{2r_0^2k_BT\ell_b} = -\frac{\partial}{\partial s}\left(g^{-(3/2)}\frac{\partial\Omega_3}{\partial s}\right) + \frac{g^{-(1/2)}\Omega_1^2\Omega_3}{2} + \frac{2\Omega_3^3}{g^{3/2}} + \frac{\Gamma}{g^{3/2}r_0^2}(\Omega_3 - \tau_N + r_0^4\Omega_3^4\tau_N), \quad (9)$$

with $\Gamma = \ell_t/\ell_b$ and the boundary condition $\partial\Omega_3/\partial s = 0$. F_3 is the force along the tangent direction of the coiled coil. Force and moment balance along the coiled-coil axis gives

$$\frac{\partial\mathbf{M}}{\partial s} = \mathbf{F}\times\mathbf{e}_3; \qquad \frac{\partial\mathbf{F}}{\partial s} = \mathbf{0}. \quad (10)$$

The coupling of the force and moment in (9) is not present in the equations for a linearly elastic rod and can lead to interesting buckling behavior and dynamics; however, this behavior lies outside the scope of this Letter and will be presented elsewhere [15].

In the absence of external moments and forces, the equilibrium configuration of the coiled coil is given by $\Omega_1 = 0$ and the solution of

$$2\Omega_3^3 + \Gamma(\Omega_3 - \tau_N)(1 - r_0^2\Omega_3^2) = 0. \quad (11)$$

The pitch of the coiled coil is $P = 2\pi/\Omega_3$. Significantly, the solution of (11) provides a more detailed relation for P than (1) by accounting for the elasticity of the α helices. The differences between the pitch calculated using (1) and (11) are shown in Fig. 2(a) for 3 different values of Γ. In the limit where $\Gamma \ll 1$, it is energetically favorable to untwist the α helices and bind them together without bending. Therefore, accounting for twist deformations of the α helices in the coiled coil predicts larger pitches than (1). X-ray structural measurements of the GCN4 leucine zipper give $h = 0.15$ nm, $r_0 = 0.465$ nm [16], and $P = 14.8$ nm [1]. Using these values and $\Gamma = 1/2$, (11) predicts $P = 15.2$ nm, whereas (1) predicts $P = 13.3$ nm. In addition, our model predicts that, for 7-residue periodicity with $\Gamma = 1/2$, the pitch should increase with r_0, whereas Eq. (1) predicts that the pitch should decrease [Fig. 2(a)]. X-ray structure data for a hybrid of GCN4 and cortexillin I shows an increase in pitch and radius compared to GCN4 [17].

To hold the coiled coil together, the residue-residue binding energy must be larger than the elastic deformation energy. Since a given residue periodicity produces a given pitch, the elastic deformation energy for a given τ_N is constant. Using Eq. (5) to calculate the elastic deformation energy per length for each of the conformations with $\ell_b = 90$ nm and $\Gamma = 1/2$, we obtain that the elastic deformation energy per length is $60.3k_BT$/nm, $7.3k_BT$/nm, and $3.1k_BT$/nm for $N = 4$, 7, and 11, respectively. In Fig. 3, we plot the total energy per length of Eq. (5) for representative values of N. To bind every 11th residue requires a minimum of $5.6k_BT$/residue. For $13 < \epsilon_R < 80$, the energy favors binding every 7th residue. Binding every 4th residue requires energies greater than $80k_BT$ per residue, which is unrealistically high. Therefore, the model predicts that stable coiled coils are formed by binding between every 11th or 7th residue, as is observed [2,9,14]. Even if synthetic α helices were engineered to have fewer than 7-residue periodicity, the binding energy would not be sufficient to form the coiled-coil structure.

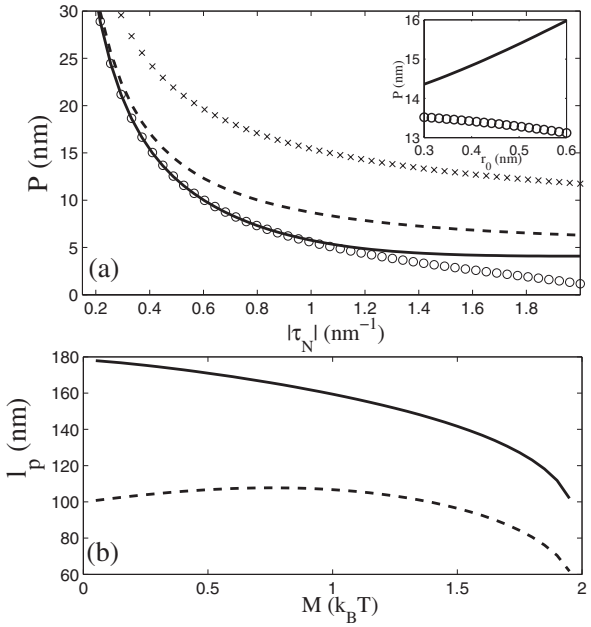

FIG. 2. (a) Pitch P vs helix torsion τ_N. P is calculated using (11) with $\Gamma = 0.05$ (×), 0.5 (dashed line), and 5 (solid line) and compared to the solution from (1) (○) with $r_0 = 0.5$ nm. The inset shows how the pitch varies with r_0. Taking into account the elasticity of the α helices, the pitch increases with r_0 (solid line), whereas (1) predicts a decrease in pitch (○). (b) The effective bend (solid line) and twist (dashed line) persistence lengths as a function of applied moment.

From the computed conformation of the coiled coil, the mechanical properties of the coiled coil can be estimated. The persistence length of a filamentary object can be defined as the bending modulus divided by k_BT, and the bending modulus is the ratio of the applied moment to the curvature. Therefore, if a moment M_1 is applied to the coiled coil, we can estimate the persistence length as ℓ_p as $M_1/k_BT\Omega_1$. Since Ω_3 and Ω_1 are coupled in Eq. (9), ℓ_p

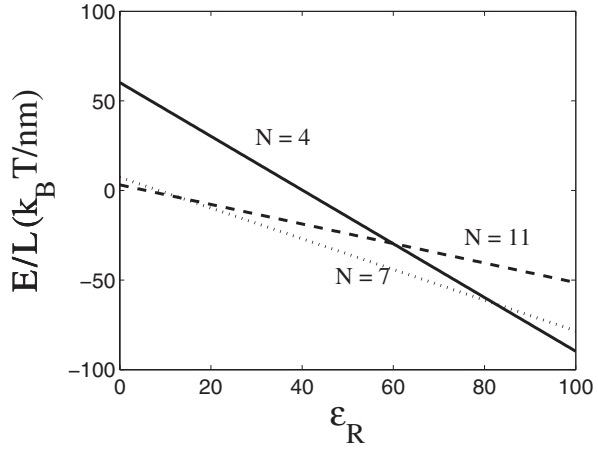

FIG. 3. The elastic energy per length as a function of the binding energy ϵ_R for $N = 4$, 7, and 11. When there is less than $13k_BT$ of binding energy per residue, 11-residue periodicity is favored. For $13 < \epsilon_R < 80$, 7th-residue periodicity is favorable.

will depend on the magnitude of the applied moment. Calculating this ratio using Eq. (9) [Fig. 2(b)], we find that ℓ_p decreases with the applied moment. The coupling between Ω_1 and Ω_3 causes the coiled coil to twist as it bends, which increases the total amount of bend, decreasing ℓ_p. Thermal fluctuations apply a moment of roughly k_BT to the coiled coil; therefore, the effective persistence length of a coiled coil should be approximately 150 nm. Experiments on the elasticity of the coiled-coil region of myosin and tropomyosin that use the same definition for the persistence length are in agreement with this result [11,12,18]. In addition, the decrease in ℓ_p with M is consistent with the strong temperature dependence of tropomyosin's persistence length [18]. Defining the effective twist persistence length as $M_3/k_BT\Omega_3$, we find that the twist persistence length also varies with applied moment [Fig. 2(b)], and we predict that the twist persistence length at room temperature is $\sim$100 nm. These estimates show that one expects that the effective persistence lengths for the coiled coil should be less than twice the persistence lengths for an α helix.

Starting with a linear elastic model of the α helix, and modeling the hydrophobic side-chain interactions as a simple attractive energy, we showed that the structural properties of α-helical coiled coils can be explained quantitatively. It is possible to predict the pitch of the supercoil for a given hydrophobic contact energy. Applying moments to coiled-coil proteins using atomic force microscopy or magnetic tweezers to measure the bending and twisting moduli would provide a method to test this model. In addition to doubled stranded coiled coils, our formalism is applicable to α-helical bundles where several helices form a supercoil. In proteins where the coiled-coil motif is present, our results can predict the deformation behavior of these motifs. Currently, molecular dynamics simulations are not able to access the dynamics of proteins on biologically relevant time scales. The agreement of our model with experimental data suggests that it is a useful method for describing coiled-coil dynamics during protein deformation. It should be noted that our discussion has been confined to geometrically perfect coiled coils where the separation between helices r_0 is constant and the hydrophobic repeat is not broken. In reality, residue side-chain packing introduces variations in r_0, and discontinuities in the hydrophobic contact occur regularly. These factors create irregular structural motifs with some variations in the coiled-coil pitch. The presence of disorder may also explain the variation in the observed coiled-coil persistence length. Our model also neglects any nonlinear behavior of the α helix, which could be important during large deformations of the coiled coil. Nonlinearity perhaps explains the diverse estimate of the coiled-coil persistence length using different experimental techniques. Finally, our results may provide new insights into the behavior of other elastic biofilaments such as actin which are composed of two polymer strands wrapped about each other.

[1] P. B. Harbury, B. Tidor, and P. S. Kim, Proc. Natl. Acad. Sci. U.S.A. **92**, 8408 (1995).
[2] P. B. Harbury *et al.*, Science **282**, 1462 (1998).
[3] S. V. Strelkov and P. Burkhard, J. Struct. Biol. **137**, 54 (2002).
[4] F. H. C. Crick, Acta Crystallogr. **6**, 685 (1953).
[5] R. D. B. Fraser and T. P. MacRae, *Conformation in Fibrous Proteins and Synthetic Polypeptides* (Academic, London, 1973).
[6] S. Choe and S. Sun, J. Chem. Phys. **122**, 244912 (2005).
[7] S. Sun, D. Chandler, A. Dinner, and G. Oster, Eur. Biophys. J. **32**, 676 (2003).
[8] G. N. Phillips, Proteins: Struct., Funct., Genet. **14**, 425 (1992).
[9] A. Lupas, Trends Biochem. Sci. **21**, 375 (1996).
[10] I. Schwaiger, C. Sattler, D. R. Hostetter, and M. Reif, Nat. Mater. **1**, 232 (2002).
[11] S. Hvidt, F. H. M. Nestler, M. L. Greaser, and J. D. Ferry, Biochemistry **21**, 4064 (1982).
[12] Appendix by J. Howard and J. A. Spudich, in T. Q. P. Uyeda, P. D. Abramson, and J. A. Spudich, Proc. Natl. Acad. Sci. U.S.A. **93**, 4459 (1996).
[13] A. E. H. Love, *A Treatise on the Mathematical Theory of Elasticity* (Dover, New York, 1944), 4th ed.
[14] P. Burkhard, J. Stetefeld, and S. V. Strelkov, Trends Cell Biol. **11**, 82 (2001).
[15] C. W. Wolgemuth and S. X. Sun (to be published).
[16] E. K. O'Shea *et al.*, Science **254**, 539 (1991).
[17] D. L. Lee *et al.*, Protein Science **12**, 1395 (2003).
[18] G. N. Phillips and S. Chacko, Biopolymers **38**, 89 (1996).